

# Anomalous Thermomechanical Softening-Hardening Transitions in Micro-oscillators

T. Sahai\*, R. Bhiladvala\*\* and A. Zehnder\*\*\*

\* Department of Theoretical and Applied Mechanics, Cornell University  
317 Kimball Hall, Ithaca 14853, NY, USA, ts269@cornell.edu

\*\* Materials Research Institute and Department of Electrical Engineering,  
The Pennsylvania State University, rbb16@psu.edu

\*\*\* Theoretical and Applied Mechanics, Cornell University, NY, USA, atz2@cornell.edu

## ABSTRACT

We report a transition in the response of a doubly-clamped micromechanical oscillator with linear inertial forcing. The experimental response of the oscillator changes, counter-intuitively, from softening to hardening on increasing the power of an incident laser beam. A novel response structure, that simultaneously displays characteristics of both softening and hardening resonances, is observed at intermediate laser powers. Using a dynamic nonlinear thermomechanical model, we show that the transition is explained by opposing responses of linear and cubic stiffness terms to temperature.

## 1 INTRODUCTION

The micromechanical oscillator used in our study is a doubly-clamped silicon nitride paddle-beam with a square plate at its center (Fig. 1 (a)). A film stack, consisting of a  $0.2\ \mu\text{m}$  thick low-stress silicon nitride layer over a  $1.5\ \mu\text{m}$  thick layer of annealed silicon oxide, is grown on silicon wafers. The stack is patterned and etched to remove the supporting sacrificial oxide layer, leaving suspended, paddle-beam structures on the silicon wafer chip.

A schematic of the experimental setup is shown in Fig. 1 (b). The chip is bonded to a piezoelectric shaker obtained from a commercial buzzer (Radio Shack 273-073) and operated in a vacuum chamber at a pressure of  $4 \times 10^{-7}$  Torr. The oscillators are driven inertially by the piezo using a signal from the tracking generator of a spectrum analyzer (Agilent E4402B). This driving signal is set to sweep over a selected frequency range. Oscillator motion is detected by interferometric modulation of a laser beam (He-Ne 633 nm), focused on the paddle using a microscope objective [2]. Laser intensity modulation is detected and amplified by an AC-coupled photodetector (New Focus 1601) and converted by the spectrum analyzer to show oscillation amplitude variation with frequency. The laser power can be continuously varied and its value recorded by a laser power detector (Graseby Optronics 52575R).

During the experiment, described in Fig. 1 (b), it is observed, while holding the driving piezo amplitude constant, that increasing the power of the sensing laser beam changes the response curve of the first bending

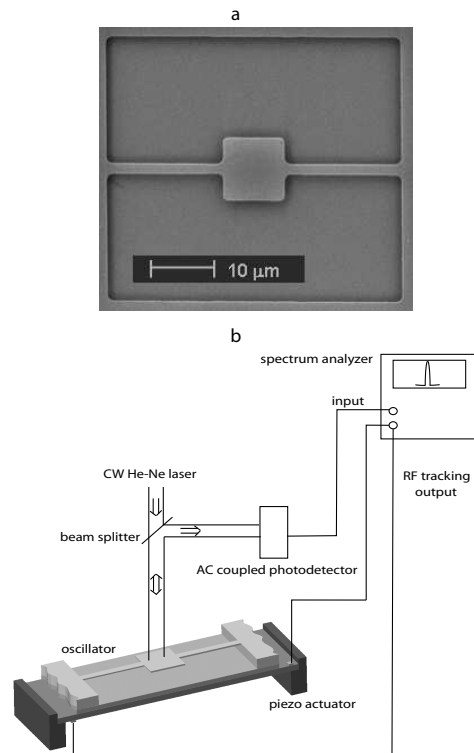


Figure 1: (a) SEM image showing suspended silicon nitride oscillator,  $0.2\ \mu\text{m}$  thick, with a  $10 \times 10\ \mu\text{m}^2$  paddle and  $18\ \mu\text{m}$  long beams. (b) The oscillator is inertially driven over a selected frequency range from the spectrum analyzer's tracking generator, using a piezoelectric actuator. Interferometric intensity variation due to the oscillator motion, sensed using the AC coupled photodetector, is converted to spectral information by the analyzer.

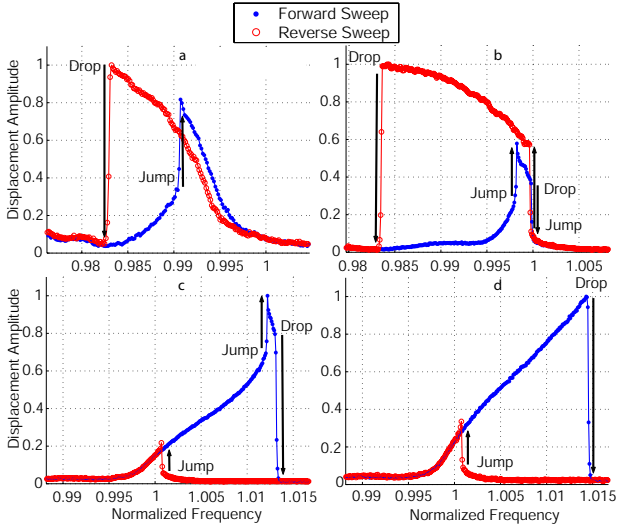


Figure 2: Experimentally obtained (a) softening curve at lowest laser power, is characterized by a shorter peak and a jump for the forward sweep direction (closed circles) and a taller peak and drop for the reverse sweep (open circles); (b) and (c) show transitional curves at increased laser powers; (d) hardening curve seen at highest laser power. Curve in (b) has the softening behavior in (a) with an added drop jump feature of (d). The laser power for curves a:b:c:d is 5 : 6 : 8 : 9 units, with one unit =  $45 \mu\text{W}$ . All plots are normalized to  $0.825 \text{ MHz}$ . The amplitudes are normalized by the height of the taller peak in each plot. The piezo forcing amplitude is held constant.

mode of oscillation from softening to hardening (Fig. 2); at intermediate laser power a transition is observed, with both softening and hardening characteristics seen in the same response curve. In earlier work, electrostatically driven oscillators have been tuned, using nonlinear forcing through selection of the DC bias voltage, to exhibit either hardening or softening behavior [5], [7] but not both. It is useful to understand the system reported here not only for its striking transitional response which has technological applications, but also for the prediction and control of nonlinearities in optically sensed motion of purely mechanical micro-oscillators with linear forcing.

## 2 MODELING

The standard Duffing equation [10], a model for oscillation of structures with constant-coefficient linear and cubic stiffness terms, cannot account for the transitions observed in our experiments. Here we show, using a thermomechanical model of the interaction of the sensing laser with the oscillator stiffness and pre-tension, that the transition arises from the opposing response of the linear and cubic stiffness terms to temperature

changes.

Large transverse deflections in a doubly-clamped beam cause it to stretch. The resulting tension increases the stiffness against further deformation, hence the beam acts as a nonlinear, hardening spring. In this model, the effect of the pretension and laser heating have also been considered. The estimated residual tensile stress of  $50 \text{ MPa}$  is found to increase the overall stiffness of the beam, while reducing the relative magnitude of deformation-induced nonlinear stiffening. As the beam heats up due to laser light absorption, this tensile stress is reduced, increasing the nonlinearity of the load-deflection response of the beam (Fig. 3).

The vibration of the paddle-beam structure is modeled by a modified Duffing equation with temperature dependent stiffness terms,

$$m\ddot{x} + c\dot{x} + k_1(T)x + k_3(T)x^3 = F_s \sin(\omega t), \quad (1)$$

where  $x$ ,  $m$ ,  $c$ ,  $T$  are the deflection, mass, damping, and temperature respectively, and  $k_1(T)$  and  $k_3(T)$  are the linear and cubic stiffnesses of the spring mass system.  $F_s$  is the piezo forcing amplitude,  $\omega$  is the piezo forcing frequency and  $t$  is time. Eq. (1) can be normalized as:

$$\ddot{z} + \frac{\dot{z}}{Q} + f(T)z + g(T)\beta_0 z^3 = M \sin(\omega t), \quad (2)$$

by dividing the entire equation by  $m$ ,  $\lambda$  (wavelength of the incident laser) and rescaling time by  $\omega_0 = \sqrt{k_1(0)/m}$ . Note, in the above equation,  $\beta_0 = k_3(0)\lambda^2/k_1(0)$ ,  $M = F_s/m\omega_0^2\lambda$ ,  $Q = m\omega_0/c$ ,  $z = x/\lambda$ ,  $f(T) = k_1(T)/k_1(0)$  and  $g(T) = k_3(T)/k_3(0)$ .

A lumped thermal mass using Newton's law of cooling models the thermal aspects,

$$\dot{T} = -BT + AP_{\text{absorbed}}, \quad (3)$$

where  $T$  is the temperature above ambient, of the micro-mechanical structure,  $A$  is the inverse of the lumped thermal capacity and  $BT$  is the rate of cooling due to conduction. As in Eq. (2), time in Eq. (3) is rescaled by  $\omega_0$ . The mass, damping, forcing amplitude and forcing frequency are assumed to be independent of  $T$ . The effects of radiation, photon pressure and Casimir forces are found to be negligible and thus not included in the model.

We need to estimate the different parameters that are part of the system of equations. To determine  $A$  and  $B$  a thermal finite element model is constructed. To simulate laser heating, a heat flux is applied at the center of the paddle. The resulting thermal response of the system yields  $A = 0.299 \text{ K}/\mu\text{W}$  and  $B = 0.004$ . Similarly,  $\beta_0$  is estimated to be  $0.875$  by using large deflection finite element analysis. The quality factor,  $Q$ , is estimated to be  $\approx 1400$  from experimental results. Forcing,  $M \approx 5 \times 10^{-5}$  is chosen such that the system is

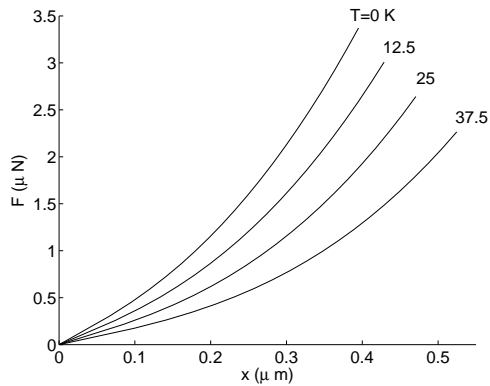


Figure 3: Spring force,  $F$  vs. static deflection,  $x$ , at different temperatures (above ambient) for a 50 MPa pretensioned beam, loaded at its center.  $F = k_1(T)x + k_3(T)x^3$ . A least squares fit on the linear and cubic stiffnesses at different temperatures gives functional approximations to  $f(T)$  and  $g(T)$ , where  $f(T) = k_1(T)/k_1(0)$  and  $g(T) = k_3(T)/k_3(0)$ .

pushed into the nonlinear regime. The material properties used for thin film silicon nitride are Young's Modulus  $E = 300 \text{ GPa}$ , Poisson's ratio  $\nu = 0.28$ , density  $\rho = 2900 \text{ kg/m}^3$ , coefficient of thermal expansion  $\alpha = 1.3 \times 10^{-6} \text{ K}^{-1}$ , thermal conductivity  $k = 3 \text{ W/(mK)}$ , specific heat capacity  $C_p = 700 \text{ J/(kgK)}$  and thermal diffusivity  $a = k/(\rho C_p) = 1.5 \times 10^{-6} \text{ m}^2/\text{s}$  [6], [4], [8]. A value of 50 MPa for beam pretension is calculated by matching the theoretical values of torsional and translational frequencies to the experimentally observed values.

The beam-substrate system forms a Fabry-Perot interferometer [3], [11].  $P_{\text{absorbed}}$  is approximated by  $P [\eta + \gamma \sin^2(2\pi(z - z_0))]$ , where  $P$  is the incident laser power. Using  $\eta = 0.133$ ,  $\gamma = 0.084$  and  $z_0 = 0.05$ , this approximation is found to agree well with theoretical calculations [11]. So Eq. (3) now becomes:

$$\dot{T} = -BT + AP [\eta + \gamma \sin^2(2\pi(z - z_0))] . \quad (4)$$

Eqs. (2) and (4) thus serve as the model equations for the first bending mode of the micromechanical oscillator. To determine  $f(T)$  and  $g(T)$ , the nonlinear deflection of pretensioned beams is calculated, as shown in Fig. 3 for different temperature [1]. We find that  $f(T) = 1 + cT$  and  $g(T) = 1 + b_1T + b_2T^2 + b_3T^3$  with  $c = -0.01$ ,  $b_1 = 1.37 \times 10^{-2}$ ,  $b_2 = 2 \times 10^{-6}$  and  $b_3 = 2 \times 10^{-5}$ , gives a good approximation for the changes in stiffness with temperature.

### 3 RESULTS

The negative sign of  $c$  gives rise to a system with a linear stiffness that decreases with increasing temperature. The nonlinear stiffness, however, increases with increasing temperature. It is the competition between

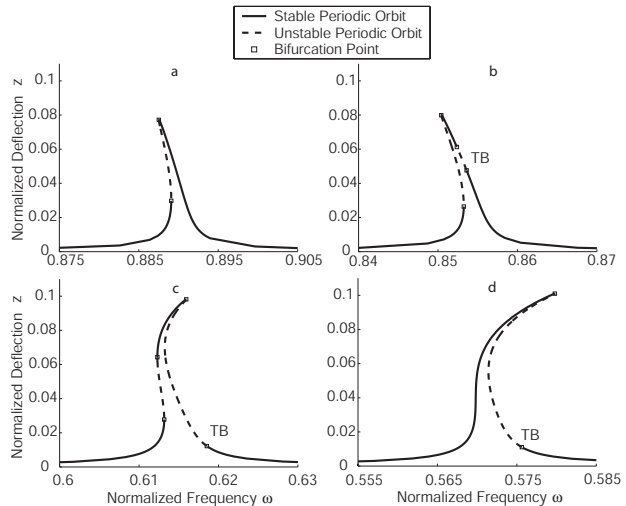


Figure 4: Maximum deflection vs. frequency at various laser powers (model predictions). Solid lines denote stable periodic motions, dotted lines denote unstable periodic motions and open squares denote bifurcation points. (a) Softening at low laser power (b) Transition from softening (c) Transition to hardening (d) Hardening at high laser power. The laser power for curves a:b:c:d is 4: 5 : 12 : 13 units, with one unit =  $5 \mu\text{W}$ . These resonance curves would give jumps and drops similar to Fig. 2. TB denotes a torus bifurcation. The periodic motion at this point loses stability and quasiperiodic motion arises.

these two terms that gives rise to the observed transitions. Using continuation algorithms [9], we compute the resonance curves numerically. At low laser powers the system is softening Fig. 4(a), whereas at high laser powers it is hardening Fig. 4(d). At intermediate laser powers (Figs. 4(b) 4(c)), the resonance curves display behavior similar to the experimental observations. At points labeled TB in Fig. 4 the periodic motion loses stability at a torus bifurcation [10] and a new quasiperiodic motion arises (not depicted in Fig. 4). Quasiperiodic motions are characterized by two incommensurate periodic components. Here, one component is at the driving frequency and the other is close to the natural frequency of the linear oscillator. The change in concavity of the resonance curve can be explained by observing that the softening in the structure arises due to a linear thermal term, the hardening response, however, arises due to a term that is nonlinear in nature.

### 4 CONCLUSIONS

The model has captured all of the features observed in the experiments. Quantitative matching will require more accurate experimental values for material properties and for post release curvature and residual stress in the fabricated structure. The predicted range of laser

power for transition is lower than the experimentally observed values. Experimental values are higher than the actual laser power incident on the oscillator as they exclude losses in some components of the optical path. As seen in Fig. 4, the predicted resonant peak shifts to lower frequencies as the laser power is increased, due to the detuning caused by the linear stiffness  $1 + cT$  term. Such large detuning is not observed experimentally, thus the parameter estimation method may be overestimating  $c$ .

The softening-hardening transition reported in this work gives a good example of how models built from first principles can be used to gain greater insight into micromechanical systems. These transitions are found to be a consequence of the interaction of the thermal stresses with the stiffness of the device. The heat from the laser changes the pretension in the beam, which changes the linear and cubic stiffnesses, but in different directions. Increasing the temperature of the oscillator decreases the linear stiffness while increasing the cubic stiffness. The competition between these two effects gives rise to the observed transitions. Using the model, oscillators could be designed to operate in the transition region. As seen in Fig. 2(b), the oscillator could be used as a mechanical realization of a bandwidth switch with sharp low and high frequency cutoffs at the jump and drop points.

## REFERENCES

- [1] R Frisch-Ray, Flexible Bars, Butterworth and Co., 1962.
- [2] D. Carr et. al., Journal of Vacuum Science and Technology, B 16,3281-3285, 1998.
- [3] K. Aubin et. al., Journal of Micromechanical Systems, 13, 1018-1026, 2004.
- [4] C. H. Mastrangelo et. al., Sensors and Actuators, 23, 856-860, 1990.
- [5] M. L. Younis and A. H. Nayfeh, Nonlinear Dynamics, 31,91-117, 2003.
- [6] B. L. Zink and F. Hellman, Solid State Communications, 129, 199-204, 2004.
- [7] W. Zhang et. al., Applied Physics Letters, 82, 130-132, 2003.
- [8] M. Gad-El-Hak, The MEMS Handbook, CRC Press, 2002.
- [9] E. J. Doedel et. al., International Journal of Bifurcation and Chaos, 1,493-520, 1991.
- [10] J. Guckenheimer and P. Holmes, Nonlinear Oscillations, Dynamical Systems and Bifurcations of Vector Fields, Springer, 1996.
- [11] E. Hecht, Optics, Addison-Wesley, 1987.